

Leucine-rich Diet Improved Muscle Function in Cachectic Walker 256 Tumor-bearing Wistar Rats

Laís Viana (✉ vianalr@unicamp.br)

State University of Campinas: Universidade Estadual de Campinas

Gabriela Chiocchetti

State University of Campinas: Universidade Estadual de Campinas

Lucas Oroy

University of Angers: Universite d'Angers

Willians Vieira

State University of Campinas: Universidade Estadual de Campinas

Carla Salgado

State University of Campinas: Universidade Estadual de Campinas

Alexandre Oliveira

State University of Campinas: Universidade Estadual de Campinas

André Viera

State University of Campinas: Universidade Estadual de Campinas

Paula Suarez

State University of Campinas: Universidade Estadual de Campinas

Lizandra Sousa

State University of Campinas: Universidade Estadual de Campinas

Bianca Castelucci

State University of Campinas: Universidade Estadual de Campinas

Silvio Consonni

State University of Campinas: Universidade Estadual de Campinas

Maria Gomes-Marcondes

State University of Campinas: Universidade Estadual de Campinas

Research

Keywords: cancer cachexia, leucine, muscle function, protein degradation

Posted Date: June 1st, 2021

DOI: <https://doi.org/10.21203/rs.3.rs-550186/v1>

License:  This work is licensed under a Creative Commons Attribution 4.0 International License.

[Read Full License](#)

Abstract

Background: Skeletal muscle atrophy occurs in several pathological conditions such as cancer, a condition termed cancer cachexia. This condition is associated with an increase in morbidity and poor treatment response, decreasing quality of life, and increased mortality in cancer patients. A leucine-rich diet could be used as a coadjutant therapy preventing muscle atrophy in cancer cachexia hosts. Besides muscle atrophy, muscle function loss is even more important to the patient's quality of life. Therefore, this study aimed to evaluate the effects of leucine-rich diet on muscle function activity of cachectic Walker 256 tumor-bearing rats and to correlate such effects with molecular pathways of muscle atrophy.

Methods: Adult Wistar rats were randomly distributed into four experimental groups. Two groups were fed with a control diet: Control (C) and Walker 256 tumor-bearing (W), and two other groups were fed with a leucine-rich diet: Leucine Control (L) and Leucine Walker 256 tumor-bearing (LW). The functional analysis (walking, behavior, and strength tests) was measured and before and after tumor inoculation. Cachexia parameters such as body weight loss, muscle and fat mass, pro-inflammatory cytokine profile, and molecular and morphological aspects of skeletal muscle were also performed.

Results: Walker 256 tumor growth led to muscle function decline, cachexia manifestation symptoms, muscle fiber cross-section area reduction, associated with the altered morphological pattern and classical muscle protein degradation pathway activation, with up-regulation of FoXO1, MuRF1, and 20S proteins. On the other hand, a leucine-rich diet improved muscle strength while reducing the decline of walking and behavior, partially improving the cachexia manifestations and preventing muscle atrophy and protein degradation in Walker 256 tumor-bearing rats.

Conclusions: A leucine-rich diet diminished muscle protein degradation and enhanced oxidative pathways, leading to better muscle functional performance.

1. Background

Skeletal muscle atrophy occurs in several pathological conditions such as cancer, a condition termed as cancer cachexia. This condition is associated with an increase in morbidity and decrease in treatment response, decreasing quality of life and increasing mortality in cancer patients (1, 2). Cancer cachexia is a multifactorial syndrome consisting of involuntary loss of body weight, especially by skeletal muscle and adipose tissue loss, reduced food intake, elevated resting energy expenditure, excess catabolism, and inflammation (3). The skeletal muscle atrophy is the main problem of cancer cachexia due to its expressive contribution to total body composition. Skeletal muscle mass counts for up to 50% of total body protein in healthy individuals (4). Striated skeletal muscle is an extremely adaptable tissue that can undergo structural and functional properties changes depending on the stimulation. The regulation of muscle mass is controlled by protein synthesis and degradation rates that should be balanced to maintain muscle mass (5). Any change, shifting the balance toward protein synthesis will lead to muscle hypertrophy, and shifting the balance toward protein degradation will lead to muscle atrophy. So far, three

main pathways of skeletal muscle protein degradation have been identified: The ubiquitin (Ub)-proteasome, cell autophagy/lysosomal and Ca²⁺-activated degradation pathways (6). Among them, Ub-proteasome system (UPS) is the main proteolytic machinery systematically activated in cachexia (7). The activation of UPS pathways is often accompanied by the presence of inflammatory mediators, including Interleukin-6 (IL-6) (8) and tumor necrosis factor alpha (TNF α) (9). Moreover, the abnormal up-regulation of muscle protein degradation is often related to the dysfunction of organelles, such as the endoplasmic reticulum (ER) (10) and mitochondria (11) which could lead to muscle function loss. Considering that skeletal muscle mass represents the most representative tissue in our body and that muscle atrophy is a severe clinical problem related to poor prognosis and higher mortality, some studies have been focused on the investigation of some potential strategies, pharmacological and non-pharmacological, that could act as a coadjuvant therapy to improve the muscle mass and function. One of the non-pharmacological strategies is nutritional supplementation, and in this regard, leucine supplementation has pride of place. Leucine is an essential, anabolic, branched-chain amino acid that can promote muscle protein synthesis by increasing mechanistic target of rapamycin (mTOR) activation (12). Additionally, leucine supplementation also affects proteolysis by inhibiting relevant catabolic transcription factors such as Forkhead Box O3 (FoxO3) (13). Furthermore, in pre-clinical studies, it is well established that using experimental models of cancer cachexia (14, 15) leucine-rich diet effectively diminishes muscle atrophy and muscle molecular and metabolic alterations related to cachexia. Although the molecular mechanisms of how leucine protects muscle cell from degradation and atrophy are described, no study until now evaluates the effects of leucine within functional analyses, which are even more important to translational perspective. Therefore, this study aimed to evaluate the effects of leucine-rich diet on muscle atrophy and functional activity of cachectic Walker 256 tumor-bearing rats and correlate such effects with molecular pathways.

2. Materials And Methods

2.1 Experimental design

Male adult Wistar rats (approximately 12 weeks old, obtained from the Animal Facilities at the State University of Campinas, UNICAMP, Brazil) were housed in collective cages under controlled environmental conditions (light and dark 12/12 h; temperature 22 \pm 2°C; and humidity 50-60%). Semi-purified diets were prepared following the recommendations of the American Institute of Nutrition (AIN-93 (16)) and according to our previous studies (17-19). The control diet contained 18% protein and was composed of 20% casein (protein source), 39.7% corn starch, 13.2% dextrin, and 10% sugar (carbohydrate sources), 7% soy oil (fat source), 5% cellulose micro fiber (fiber source), 3.5% salt mix, 1.0% vitamin mix, 0.3% cysteine, and 0.25% choline. The leucine-rich diet also contained 18% protein and was composed of the same amounts of casein, fat, fiber, salt, vitamin mix, cysteine, and choline as the control diet. The addition of 3% leucine was followed by a 1% reduction in corn starch (38.7%), dextrin (12.2%), and sugar (9%). Whiting those adjustments, both diets, control and leucine, were normoproteic, isocaloric, and normolipidic. The widely used model of cancer cachexia, Walker 256 carcinosarcoma (20) was used in this study. Cell suspension (2.5 \times 10⁶ viable cells) of Walker 256 cells were injected subcutaneously into

the right flank of the rats. The tumor inoculation and diet administration started on the same day (Figure 1).

The animals were randomly distributed into four experimental groups. Two groups were fed with a control diet: Control (C) and Walker 256 tumor bearing (W), and two other groups were fed with a leucine-rich diet : Leucine Control (L) and Leucine Walker 256 tumor-bearing (LW). The minimal number of animal per group was 6. The animals were monitored daily, weighed 3 times/week and given food and water ad libitum. Food intake was measured once per week, and the functional activities were accessed one week before (to assess the health condition) and after approximately 18 days after tumor and diet administration (pre-agonic moment) (Figure 1).

The final endpoint criteria (pre-agonic moment) utilized in the present study were determined based on the data derived from daily observation of discomfort symptoms such as piloerection, diarrhea or constipation, hunched posture, tremors, closed eyes and red tears (chromodacryorrhea). These symptoms were based on the indicators of quality of life proposed by Betancourt et al. [15]. At the endpoint moment (~ 18 days following tumor inoculation), rats were killed by decapitation, and different body tissues, such as spleen, perirenal fat and skeletal muscle (musculus tibialis anterior) were removed and weighed (Figure 1). The tibia length of each animal was used to normalize their corresponding tissues weights. Muscle samples were frozen directly in liquid nitrogen and stored at -80°C for further gene and protein expression analysis. Also, muscle fragments were also immediately fixed in 2.5 % glutaraldehyde and 2.5% paraformaldehyde in sodium cacodylate buffer (0.1M) at pH 7.4 and CaCl_2 (3mM) for 24 h at 4°C before being processed for electron microscopy analysis. Additional muscle samples were fixed in 4% paraformaldehyde for light microscopic assay. The general guidelines of the United Kingdom Coordinating Committee on Cancer Research (UKCCCR), 1998 [10] regarding animal welfare were followed, and the experimental protocol was approved by the Institutional Committee for Ethics in Animal Research (CEEA/IB/UNICAMP, protocol # 4289-1).

2.2 Muscle Functional Analyses

Catwalk walking test

Catwalk walking test (Noldus Inc., Wageningen, Netherlands) consists of an automated tool that quantifies gait parameters. Rats were placed in an illuminated-walkway glass-floor with a video camera (Gevicam GP-3360; Gevicam Inc., CA, USA). The camera positioned under the walkway at a distance of 56 cm recorded the paws prints automatically by using the CatWalkTM XT10.6 software, as the animal crossed the pathway in a calibrated 20 x 10 cm length lane. The maximum intensity measurements were analyzed, which represent the intensity of the complete paw. Besides, the maximum contact area (cm^2) was accessed, which corresponds to the max area of a paw that comes into contact within the glass-floor and the print area (cm^2). The surface area of the complete paw print of both tumor-bearing groups (W and LW) was compared with the gait patterns at the initial time point (pre-tumor inoculation) and the pre-agonic moment (~18 days after tumor inoculation). All experimental animals used were acclimated to the test one week before the experiment started. The software detects all paws during natural gait, recording

all right front (RF); left front (LF); – right hind (RH) and left hind (LH) paws. The average of forepaws (RF and LF) was considered as forelimb, and the average of hind paws (RH and LH) were considered hindlimb.

Behavior test (Video recording system and analysis)

The animal behavior was accessed by night vision cameras placed in front of each individual cage at an adequate height. The cameras recorded all rats activities during their nocturnal behavior. The video recording system commenced one week before the experiment started. Video files were analyzed using the video tracking software EthoVisionXT12 (Noldus Information Technology, Netherlands) to access the total distance covered (cm), the average velocity (cm.s⁻¹) and the time spent in movement (s) of both tumor-bearing groups (W and LW). All data from tumor groups were compared to their behavior at the initial time point (pre-tumor inoculation) and at the pre-agonic moment (~18 days after tumor inoculation) and also compared to control groups.

Grip Strength test

The grip strength test was performed randomly in all experimental groups at the beginning and endpoint moment of the experiment to access force measurement. The equipment use procedures followed the manufactures' instructions (BIOSEB's Grip Strength Test), and was always operated by the same researcher during the morning period. The animals were placed in the grip strength room 15 minutes before the test to acclimate them to the environment. Briefly, rats were held by the tail and lowered towards the grip strength meter. The animals were allowed to grab the metal grip and were then pulled backwards in the horizontal plane. The force applied to the grid just before it loses grip was recorded as the peak tension. Measurements were repeated 10 times for each animal, and it was recorded in grams and then normalized by the tibia length of each individual animal.

Light Microscopy

Muscle samples were removed from animals and immersed in a fixative solution (4% paraformaldehyde in 0.1 M phosphate-buffered saline (PBS), pH 7.4) for 24 hours at 4°C. Then, tissues were dehydrated in graded concentrations of alcohol, embedded in historesin (Leica Microsystems, Heidelberg, Germany) and sectioned at a width of 3 µm. The sections were mounted on slides and stained with hematoxylin-eosin-floxin. The sections were then examined for image analysis of cross-sectional area using a Nikon Eclipse E800 light microscope (Nikon Corporation, Tokyo, Japan). The cross-sectional area of myofibers was measured using Image Pro-Plus Premium software (v.3.01, Media Cybernetics, Silver Spring, MD, USA) after capturing the image in a Leica microscope (Leica DMLM, Wetzlar, Germany) using a 20× magnification.

Transmission Electron Microscopy

The transmission electron microscopic was accessed as briefly described: the skeletal muscle tissue was immersed in a fixative solution consisting of 2.5 % glutaraldehyde and 2.5% paraformaldehyde in sodium

cacodylate buffer (0.1M) at pH 7.4 and CaCl₂ (3mM) for 24 h at 4°C. Then, tissue samples were rinsed with cacodylate buffer/CaCl₂ and were post-fixed in 1% OsO₄ in sodium cacodylate buffer (0.1M), CaCl₂ (3mM), and potassium ferrocyanide solution (0.8%) for 1 h on ice. Following, tissue samples were washed with milli-Q water and stained with uranyl acetate (2%) overnight at 4 °C. Then, tissue samples were washed in milli-Q water and dehydrated in an ethanol gradient. The samples were embedded in Epon 812 resin. Resin polymerization was controlled in an incubator (60°C) for 72h. Ultra-thin sections were stained with uranyl acetate, and lead citrate then observed in a transmission electron microscope LEO 906 (Zeiss), operated at 60 kV.

Serum cytokines assay

The serum cytokine (IL-6, TNF, IL-10) profile was measured by Luminex assay using a specific kit (Rat Premixed Multi-Analyte kit) from R&D Systems® (Minneapolis, USA) following the manufacturer's technical procedures.

Quantitative RT-PCR

Total RNA from the tibialis anterior muscle tissue was extracted with TRIZOL® reagent (Invitrogen) following the manufacturer's instructions. The quality of the RNA samples was examined at 260/280 nm and 260/230 nm with a UV spectrophotometer (Nanovue Spectrophotometer 28923215 Ge BioSciences, USA). cDNA was produced using a high capacity cDNA reverse transcription kit (Applied Biosystems®, USA) containing Multiscript™ Reverse Transcriptase. cDNA synthesis was performed on 1 µg of RNA at 42 °C. Real-time reactions were performed using standard methods (ABI Prism 7500 Sequence Detection System; Applied Biosystems, Foster City, USA) and qPCR analysis was normalized to GAPDH. The genes evaluated using qPCR were FoxO3 (forward primer 5'- AACTTTGAC TCC CTC ATC TC -3' and reverse primer 5'- TTT TCT CTG TAG GTC TTC GG - 3'), IL-6 (forward primer 5'- ACT CAT CTT GAA AGC ACT TG -3' and reverse primer 5'- GTC CAC AAA CTG ATA TGC TTA G -3'), Ubiquitin (forward primer 5'- CAA GCT CAG TCT TTT GCC TCA GA -3' and reverse primer 5'- GGA TCG GCG GGT AAT GAA G -3'), COX5a (forward primer 5'-TGTTGGCTATGATCTGGTTCC-3' and reverse primer 5'-TTATGAGGTCCTGCTTTGTCC-3'), CS (forward primer 5'-TATGGCATGACGGAGATGAA-3' and reverse primer 5'-CATGGACTTGGGCCTTTCTA-3'), and GAPDH forward primer 5'- CCA TGG AGA AGG CTG GG -3' and reverse primer 5'- CAA AGT TGT CAT GGA TGA CC -3').

Western blotting

Samples of tibialis anterior muscle biopsies were lysed in RIPA buffer (150 mM NaCl, 25 mM Tris-Cl, pH 7,4, 0,1% SDS, 1% NP-40, 0,5% sodium deoxycholate) and supplemented with protease and phosphatase inhibitors. After protein extraction protocol, protein concentration was measured by the bicinchoninic acid (BCA) method, following the manufacturer's instructions (Pierce™ BCA Protein Assay Kit, Sigma Aldrich, Poole, UK). The proteins (40 µg) were separated by electrophoresis, transferred to nitrocellulose membranes and stained proteins with Ponceau S. After that, the membranes were incubated with primary antibodies against FoxO1 (CellSignaling, 1:1000), MurF (CellSignaling 1:1000), 20S (CellSignaling

1:1000), OXPPOS (Abcam 1:1000), and GAPDH (CellSignaling 1:1000) as a loading control. After that, the membranes were probed with secondary antibodies conjugated with peroxidase, and bands were visualized using a chemiluminescent reagent (ThermoFisher Scientific). The membrane images were captured using an image system (Amersham Imager 600, GE Healthcare), and band volume quantitation was quantified.

Statistical Analysis

Data are expressed as mean \pm SEM. Differences between 3 or more groups were analyzed by variance test ANOVA, followed by Tukey post hoc test and by t-test for comparison among 2 groups. For correlation analysis, the Pearson coefficient was calculated. For all statistical analyses, $P < 0.05$ was considered significant. The statistical analyses were performed using the software Graph Pad Prism 6.0 (Graph-Pad Software, Inc).

3. Results

3.1 Walker 256 tumor growth altered muscle function. Leucine-rich diet improved muscle strength while reducing the walking and behavior decline

Cachexia state imposed by the Walker 256 tumor growth led to an impaired muscle function, which was accessed in this present study by walking, behavioral and strength tests. The Catwalk test revealed that the walking pattern was significantly altered at the endpoint moment in both W and LW groups (Figure 1). Despite not having completely prevented functional decline, the leucine-rich diet minimized this decay in some of the analyzed parameters. The maximum contact area (Figure 2a) and the print area (Figure 2b) of forelimb paws were significantly decreased ($P < 0.01$; less 30.2% and 30%, respectively) at the endpoint moment compared to the initial moment in W group, but these parameters remained unchanged in LW. For the hindlimb paws, both W and LW presented decreased maximal contact and print areas but in a more significant dimension in W group ($P < 0.01$; 50.8% and 49.6%, respectively) than in LW group ($P < 0.05$; 34.7% and 32.9%) (Figures 2a and 2b). In the same line, the maximum intensity of the fore and hindlimb were decreased in both W and LW groups after ~ 18 days of tumor inoculation, but for W group this reduction was more expressive (P -value < 0.001 , 5.8% and 6.8% for fore and hindlimbs, respectively) than in LW group (4.3% ($P < 0.01$) and 3.3% ($P < 0.05$) for fore and hindlimbs, respectively) (Figure 2c).

Similarly, the behavior analysis showed that Walker 256 tumor evolution negatively impacted the mobility of tumor-bearing rats. The distance moved (Figure 3a), velocity and time moving (Figure 3b and c) reduced significantly in about 31.7%, 50.0% and 32.8%, respectively, in W group in comparison to C group. Although the time moving diminished during tumor evolution, the LW improved 14.3% compared to W group (Figure 3d). On the other hand, the distance moved (Figure 3a), and the velocity (Figure 3b) remained unchanged in LW group in comparison to the control groups. Corroborating with the preservation of total distance moved and velocity, the force measurement, accessed by grip strength, was also preserved in the LW group but significantly decreased, around 42%, in W compared to C group (Figure 3d).

3.2. Leucine-rich diet partially improved cachexia manifestations in tumor-bearing rats

The muscle function decline in Walker 256 tumor-bearing rats was accompanied by cachexia symptoms normally observed in cancer-cachectic hosts. Food intake and the body weight reduced in W and LW groups (Figure 4a and 4b). Although being also decreased in LW group, the body weight gain tended to be higher than the W group ($P=0.06$ - Figure 4b). Additionally, the spleen mass was extremely increased in both tumor-bearing groups (Figure 4c), reflecting the inflammatory state imposed by cancer cachexia. The adipose tissue was also depleted in the W but preserved in LW group (Figure 4c). Despite having a higher content of IL-6 and TNF α , the leucine supplementation led a little blunt in inflammatory alterations, as LW group had a 20% less TNF α level, and 30% less increase in IL-6 content compared to W group (Figures 4d and 4e). Although the ratio of pro-inflammatory by anti-inflammatory cytokines, TNF- α /IL-10 and IL-6/IL-10, was also increased in both tumor-bearing groups, despite being a small effect, the leucine nutritional stimuli minimized this enhance around 15% in LW group (Figures 4f and 4g). Even with this inflammatory state, the perirenal adipose tissue and tibialis anterior (TA) muscle mass remained unchanged in the LW group and significantly reduced in W compared to C group (Figures 4c and 5a). Besides, the correlation between TA muscle mass and IL-6 showed that higher pro-inflammatory cytokine was inverse to muscle mass, independently of the nutritional scheme ($r = -0.4062$, $P = 0.0084$) (Figure 4h). As the same profile, the TNF α content was inversely correlated to TA, with a tendency to be significant ($r=-0.3053$ and $P = 0.0745$) (Figure 4i).

3.3 Walker 256 tumor growth led to muscle damage which was prevented by leucine-rich diet

The tibialis anterior muscle mass reduced 29.9 % only in W group in relation to C and L groups (Figure 5a). In this same way, myofiber cross-sectional area (CSA) was preserved in LW and significantly reduced in W compared to C group (Figure 5b and 5d). The myofiber atrophy measured by CSA was accompanied by qualitative/visual ultra-morphological muscle changes (Figure 5d and 5e).

3.4 Leucine-rich diet was able to prevent muscle protein degradation and oxidative stress in Walker 256 tumor-bearing rats

It is also well established that protein degradation is upregulated in cachectic muscle. We evaluated the expression of key genes related to muscle catabolism and found that the expression of Il-6, FoXO3 and ubiquitin genes was increased in both W and LW groups (Figure 6a). Although the increase in catabolic genes was evident independently of leucine supplementation, the increased expressions of FoXO1, MuRF1 and 20S happened only in W group (Figure 6b-d, respectively). The mitochondrial oxidative metabolism was also investigated. The gene expression of Cox5a, which is a mitochondrial function-associated gene, and CS, related to oxidative metabolism, were decreased only in W compared to C group, and remained unchanged in the LW group (Figure 6e). The same pattern was observed at the protein expression of complex V (CV) and II (CII) of the mitochondrial respiratory chain (Figure 6f and 6g, respectively). Both CV and CII protein expression were significantly reduced only in W group, while the leucine-rich diet led to the maintenance of these parameters, remaining unchanged in LW group compared to C group (Figure 6f and 6g).

Discussion

The present study shows the importance of a leucine-rich diet as a coadjutant treatment in an experimental model of cancer cachexia with important findings of functional muscle activity in tumor-bearing rat subjected to a 3% nutritional leucine supplementation. Cancer cachexia is characterized by a significant involuntary body weight loss, mainly related to skeletal muscle loss (3, 21). The muscle atrophy is induced by tumor and host released factors that lead to an inflammatory state, activating proteolysis and inhibiting protein synthesis. In addition to the loss of muscle mass, the cachectic patient also presents a significant reduction in muscle function, which is related to less quality of life. Although some molecular mechanisms of how leucine protect muscle cell from Walker 256 tumor evolution have already been described, no study so far has evaluated the effects of leucine within functional analyses, being even more important from a translational perspective. Therefore, this study evaluated the effects of leucine-rich diet on muscle function activity of cachectic Walker 256 tumor-bearing rats and correlated such effects with molecular pathways of muscle atrophy. As expected, Walker-256 tumor growth jeopardized muscle function, declining walking, behavior and strength tests, as well as morphometric parameters such as body weight and skeletal muscle loss and anorexia. Our results showed that leucine-rich diet improved muscle strength while reducing the walking and behavior decline affected by tumor evolution. Similar results were recently found in a clinical study performed by Martinez and colleagues (2020), where the administration of leucine significantly improved some functional performance measured by walking time and improved lean mass index in sarcopenic elderly individuals. Furthermore, the authors found that the leucine-treated group improved the respiratory muscle function significantly, measured by the maximum static expiratory force compared to the placebo. They concluded the study by saying that the use of leucine supplementation can have some beneficial effects on sarcopenia and could be considered for the treatment of sarcopenia in older individuals (22). Another study found beneficial effects of leucine, partially protecting muscle health during relatively brief periods of physical inactivity in muscle function of bed rest on muscle metabolism, mass, and function in middle-aged adults (23). A study performed by VanderVeen and colleagues (24) showed that a slow-fatigable contractile phenotype is developed during the progression of cachexia and that this fatigability phenotype is directly related to increased muscle inflammatory signaling. According to this study, we also found a decrement in skeletal muscle function during cachexia evolution that was highly impacted in the advanced stages of cachexia, accompanied by smaller myofiber size. Furthermore, we also found that an upregulated inflammatory signaling accompanied these muscle function and morphology changes. In this point of view, some of the cachectic symptoms such as higher pro-inflammatory IL-6 cytokine content, as observed in the tumor-bearing group, were diminished by leucine-rich diet, showing the nutritional supplementation effect. Besides being protective for skeletal muscle function, mass and structure, leucine could preserve the fat mass in LW group. The white adipose tissue (WAT), as well as skeletal muscle, is usually depleted with cachexia. The adipose tissue spoliation is an important contributor to cachexia since WAT synthesizes many pro-inflammatory cytokines, contributing to systemic inflammation (25). Moreover, some evidence showed that WAT alterations precede muscle wasting (26, 27). The present study showed interesting findings that leucine supplementation likely suggests an amelioration

of the inflammatory state, maintaining unchanged the perirenal adipose tissue and tibialis anterior muscle mass in the LW group. Indeed, the improvement in muscle function and muscle fiber size as observed in leucine-supplemented Walker-256 group after approximately 18 days of tumor evolution was expected, even despite being smaller, because we observed minimization of structural muscle changes since the leucine-rich diet prevented sarcomere atrophy. Thus, this may suggest that the leucine-rich diet could preserve the muscle contraction capacity and consequently muscle function, maintaining the functional parameters. Our previous results showed that muscle energy production was preserved in leucine treated tumor-bearing animals and in *in vitro* muscle cells treated with tumor factors, improving the muscle mitochondrial oxidative metabolism (15). Knowing that proteolytic pathway is highly expressed in cachectic muscle and that the activation of this pathway leads to muscle atrophy, we hypothesized that leucine-rich diet decreases, even partially, the activation of proteolytic/catabolic pathways. Here, we found that even increased the gene expression of Il-6 and FoxO3 in both tumor-bearing groups; leucine supplementation blunted the expression of key catabolic related proteins as the increased expression of FoxO1, MuRF1 and 20S, only observed in the tumor-bearing group without nutritional supplementation. It is well established that FoxOs transcription factors are overexpressed in cachectic muscles [7]. It is also known that leucine enhances muscle protein synthesis (28-30). However, in the present study the main protein synthesis pathway, e.g. mTOR pathway, was not altered in cachectic Walker 256 tumor-bearing rats, so leucine-rich diet did not affect this pathway (data not shown). Interestingly, in addition to genes linked with proteolytic/catabolic pathways, more than 10% of the atrophy-related genes are directly involved in energy production. Furthermore, several genes coding for essential enzymes in glycolysis and oxidative phosphorylation are coordinately suppressed in atrophying muscles (31). These points suggest that alterations in mitochondria and the mitochondrial network morphology can have potentially deleterious consequences for maintaining muscle mass and function. A study performed by Fontes-Oliveira and colleagues (11) found that cancer cachectic muscle undergoes profound morphological changes, which are visualized mainly in alterations in sarcoplasmic reticulum and mitochondria. These alterations are linked to pathways that can account for inefficiently energy source associated with cancer cachexia. According to this study, we found profound morphological alterations in mitochondria and calcium release units that could be related to deficient energy production, as our previous results (15). We observed that the density of mitochondria decreased in skeletal muscle of W group, which implicated lower OXPHOS capacity and consequently lower energy (ATP) production and finally impaired muscle function. As interestingly showed here, the leucine-treated group had no decreased mitochondrial density (verified as a qualitative analysis of MET images), possibly showing that the leucine-rich diet could improve the OXPHOS capacity in this tumor-bearing host, as shown previously in our results (15). This possibility is supported by the fact that acetyl-CoA, which is one of the final catabolic products of leucine metabolism, can be directly consumed by mitochondria through the TCA cycle (32), favoring OXPHOS. We also verified that the mitochondrial oxidative metabolism was preserved in the leucine-treated group (LW). The mitochondrial function-associated gene expression of Cox5a, and citrate synthase, directly related to oxidative metabolism, were decreased only in W, while was unchanged in LW group. The same pattern was observed at protein expression of complex V (CV) and II (CII) of the mitochondrial respiratory chain, which was maintained by the leucine-rich diet in these tumor-

bearing rats. Other studies have shown that leucine can increase OXPHOS capacity and mitochondrial biogenesis in skeletal muscle cells (15, 33-36). The study performed by Vaughan and colleagues (37) evaluated the effects of leucine treatment on oxidative and glycolytic metabolism in human and murine skeletal muscle cells. The authors also observed a significant reduction in glycolytic metabolism and also on lactate export in leucine-treated cells. Therefore, Vaughan and colleagues (37) concluded that leucine could potentially induce an oxidative profile by increasing the oxidative capacity in skeletal muscle cells.

In the meantime, it is important to raise some limitations of the present study. We carried out all the evaluations before the tumor injection and at the endpoint (pre-agonic), in which cachexia is evident and almost terminal. Considering that anorexia is sometimes starting on the 14th day of tumor growth, performing the assessments also at this point would also add some specific data about the cachexia stage. Also, leucine-rich diet administration was initiated on the same day of tumor inoculation, inferring to be the diagnostic time for a patient, although it could be a limitation for a translational value of the results. Maybe, future studies should consider starting the diet administration at different points of tumor evolution as a treatment outcome. It is also important to highlight that new studies should investigate the mechanism of how leucine improves muscle function, evaluating both muscle and neural function and specifically the neuromuscular junction to better understand the benefits of leucine.

Conclusion

Summing up, here we have presented some specific positive points of nutritional supplementation with leucine and some beneficial effects over the cachectic state in this experimental Walker 256 tumor model. A leucine-rich diet diminished the expression of muscle catabolic proteins, such as FoXO1, MuRF1, and 20S, and maintained the normal levels of important oxidative proteins as CV and CII of the mitochondrial respiratory chain. Altogether, these molecular effects of a leucine-rich diet led to better muscle functional performance in this experimental tumor model. Considering that muscle function is very important to translational perspective our study showed that a leucine rich-diet could be beneficial to cancer cachectic patients and should be considered for clinical studies to prove its potential beneficial effect in humans.

Abbreviations

FoXO1: Forkhead Box O1

MuRF1: Muscle-specific RING-finger protein 1

Ub: Ubiquitin

UPS: Ub-proteasome system

IL-6: Interleukin-6

TNF α : Tumor necrosis factor alpha

ER: endoplasmic reticulum

mTOR: mechanistic target of rapamycin

FoxO3: Forkhead Box O3

AIN: American Institute of Nutrition

IL-10: Interleukin-10

CV: complex V

CII: complex II

TA: tibialis anterior

COX 5a: cyclooxygenase 5a

CS: citrate synthetase

Declarations

Ethics approval

The experimental protocol of the present study was approved by the Institutional Committee for Ethics in Animal Research (CEEA/IB/UNICAMP, protocol # 4289-1).

Consent for publication

Not applicable

Availability of data and materials

The data and materials used during the current study are available from the corresponding author on a reasonable request.

Funding

This research was funded by CAPES, CNPq grants numbers: 302863/2013-3; 302425/2016-9; 301771/2019-7 and FAPESP grants numbers: 2012/06955-0; 2014/13334-7; 2015/21890-0; 2017/02739-4; 2019/14803-4.

Competing interests

The authors declare that they have no competing interests.

Authors' contributions

Conceptualization L.R.V and M.C.C.G.M.; Investigation L.R.V, G.M.C. and M.C.C.G.M.; Resources M.C.C.G.M.; Validation, L.R.V. G.M.C. and M.C.C.G.M.; Formal Analysis L.R.V. G.M.C. and M.C.C.G.M.; Writing-Original Draft, L.R.V. G.M.C. and M.C.C.G.M. ; Supervision, M.C.C.G.M.; Funding Acquisition L.R.V and M.C.C.G.M. All authors reviewed the manuscript prior to submission.

Acknowledgements

We thank Rogério Willians dos Santos for assistance with animal care. Serum analyses kits were kindly donated by Bioclin-Quibasa, Brazil, and the L-leucine and L-cistine were kindly provided by Ajinomoto Brasil.

References

1. Romanello V, Sandri M. Mitochondrial Quality Control and Muscle Mass Maintenance. *Front Physiol.* 2015;6:422.
2. Penna F, Ballaro R, Beltra M, De Lucia S, Garcia Castillo L, Costelli P. The Skeletal Muscle as an Active Player Against Cancer Cachexia. *Front Physiol.* 2019;10:41.
3. Baracos VE, Martin L, Korc M, Guttridge DC, Fearon KCH. Cancer-associated cachexia. *Nat Rev Dis Primers.* 2018;4:17105.
4. Muller MJ, Geisler C, Pourhassan M, Gluer CC, Bopsy-Westphal A. Assessment and definition of lean body mass deficiency in the elderly. *Eur J Clin Nutr.* 2014;68(11):1220–7.
5. Anthony TG. Mechanisms of protein balance in skeletal muscle. *Domest Anim Endocrinol.* 2016;56 Suppl:S23–32.
6. Williams A, Sun X, Fischer JE, Hasselgren PO. The expression of genes in the ubiquitin-proteasome proteolytic pathway is increased in skeletal muscle from patients with cancer. *Surgery.* 1999;126(4):744–9; discussion 9–50.
7. Attaix D, Combaret L, Bechet D, Taillandier D. Role of the ubiquitin-proteasome pathway in muscle atrophy in cachexia. *Curr Opin Support Palliat Care.* 2008;2(4):262–6.
8. White JP, Puppa MJ, Gao S, Sato S, Welle SL, Carson JA. Muscle mTORC1 suppression by IL–6 during cancer cachexia: a role for AMPK. *Am J Physiol Endocrinol Metab.* 2013;304(10):E1042–52.
9. Li YP, Schwartz RJ, Waddell ID, Holloway BR, Reid MB. Skeletal muscle myocytes undergo protein loss and reactive oxygen-mediated NF-kappaB activation in response to tumor necrosis factor alpha. *FASEB J.* 1998;12(10):871–80.
10. Bohnert KR, Gallot YS, Sato S, Xiong G, Hindi SM, Kumar A. Inhibition of ER stress and unfolding protein response pathways causes skeletal muscle wasting during cancer cachexia. *FASEB J.* 2016;30(9):3053–68.
11. Fontes-Oliveira CC, Busquets S, Toledo M, Penna F, Paz Aylwin M, Sirisi S, et al. Mitochondrial and sarcoplasmic reticulum abnormalities in cancer cachexia: altered energetic efficiency? *Biochim Biophys Acta.* 2013;1830(3):2770–8.

12. Katsanos CS, Kobayashi H, Sheffield-Moore M, Aarsland A, Wolfe RR. A high proportion of leucine is required for optimal stimulation of the rate of muscle protein synthesis by essential amino acids in the elderly. *Am J Physiol Endocrinol Metab.* 2006;291(2):E381–7.
13. Pereira MG, Baptista IL, Carlassara EO, Moriscot AS, Aoki MS, Miyabara EH. Leucine supplementation improves skeletal muscle regeneration after cryolesion in rats. *PLoS One.* 2014;9(1):e85283.
14. Cruz BL, da Silva PC, Tomasin R, Oliveira AG, Viana LR, Salomao EM, et al. Dietary leucine supplementation minimises tumour-induced damage in placental tissues of pregnant, tumour-bearing rats. *BMC Cancer.* 2016;16:58.
15. Cruz B, Oliveira A, Viana LR, Lopes-Aguiar L, Canevarolo R, Colombera MC, et al. Leucine-Rich Diet Modulates the Metabolomic and Proteomic Profile of Skeletal Muscle during Cancer Cachexia. *Cancers (Basel).* 2020;12(7).
16. Reeves PG, Nielsen FH, Fahey GC, Jr. AIN–93 purified diets for laboratory rodents: final report of the American Institute of Nutrition ad hoc writing committee on the reformulation of the AIN–76A rodent diet. *J Nutr.* 1993;123(11):1939–51.
17. Viana LR, Gomes-Marcondes MC. Leucine-rich diet improves the serum amino acid profile and body composition of fetuses from tumor-bearing pregnant mice. *Biol Reprod.* 2013;88(5):121.
18. Viana LR, Canevarolo R, Luiz AC, Soares RF, Lubaczeuski C, Zeri AC, et al. Leucine-rich diet alters the (1)H-NMR based metabolomic profile without changing the Walker–256 tumour mass in rats. *BMC Cancer.* 2016;16(1):764.
19. Viana LR, Tobar N, Busanello ENB, Marques AC, de Oliveira AG, Lima TI, et al. Leucine-rich diet induces a shift in tumour metabolism from glycolytic towards oxidative phosphorylation, reducing glucose consumption and metastasis in Walker–256 tumour-bearing rats. *Sci Rep.* 2019;9(1):15529.
20. Ballaro R, Costelli P, Penna F. Animal models for cancer cachexia. *Curr Opin Support Palliat Care.* 2016;10(4):281–7.
21. Argiles JM, Busquets S, Stemmler B, Lopez-Soriano FJ. Cancer cachexia: understanding the molecular basis. *Nat Rev Cancer.* 2014;14(11):754–62.
22. Martinez-Arnau FM, Fonfria-Vivas R, Buigues C, Castillo Y, Molina P, Hoogland AJ, et al. Effects of Leucine Administration in Sarcopenia: A Randomized and Placebo-controlled Clinical Trial. *Nutrients.* 2020;12(4).
23. English KL, Mettler JA, Ellison JB, Mamerow MM, Arentson-Lantz E, Pattarini JM, et al. Leucine partially protects muscle mass and function during bed rest in middle-aged adults. *Am J Clin Nutr.* 2016;103(2):465–73.
24. VanderVeen BN, Hardee JP, Fix DK, Carson JA. Skeletal muscle function during the progression of cancer cachexia in the male Apc(Min/+) mouse. *J Appl Physiol (1985).* 2018;124(3):684–95.
25. Batista ML, Jr., Olivian M, Alcantara PS, Sandoval R, Peres SB, Neves RX, et al. Adipose tissue-derived factors as potential biomarkers in cachectic cancer patients. *Cytokine.* 2013;61(2):532–9.
26. Bing C, Bao Y, Jenkins J, Sanders P, Manieri M, Cinti S, et al. Zinc-alpha2-glycoprotein, a lipid mobilizing factor, is expressed in adipocytes and is up-regulated in mice with cancer cachexia. *Proc*

- Natl Acad Sci U S A. 2004;101(8):2500–5.
27. Bing C, Russell S, Becket E, Pope M, Tisdale MJ, Trayhurn P, et al. Adipose atrophy in cancer cachexia: morphologic and molecular analysis of adipose tissue in tumour-bearing mice. *Br J Cancer*. 2006;95(8):1028–37.
 28. Kimball SR, Shantz LM, Horetsky RL, Jefferson LS. Leucine regulates translation of specific mRNAs in L6 myoblasts through mTOR-mediated changes in availability of eIF4E and phosphorylation of ribosomal protein S6. *J Biol Chem*. 1999;274(17):11647–52.
 29. Anthony JC, Yoshizawa F, Anthony TG, Vary TC, Jefferson LS, Kimball SR. Leucine stimulates translation initiation in skeletal muscle of postabsorptive rats via a rapamycin-sensitive pathway. *J Nutr*. 2000;130(10):2413–9.
 30. Dardevet D, Sornet C, Balage M, Grizard J. Stimulation of in vitro rat muscle protein synthesis by leucine decreases with age. *J Nutr*. 2000;130(11):2630–5.
 31. Lecker SH, Jagoe RT, Gilbert A, Gomes M, Baracos V, Bailey J, et al. Multiple types of skeletal muscle atrophy involve a common program of changes in gene expression. *FASEB J*. 2004;18(1):39–51.
 32. Adeva-Andany MM, Lopez-Maside L, Donapetry-Garcia C, Fernandez-Fernandez C, Sixto-Leal C. Enzymes involved in branched-chain amino acid metabolism in humans. *Amino Acids*. 2017;49(6):1005–28.
 33. Sun X, Zemel MB. Leucine modulation of mitochondrial mass and oxygen consumption in skeletal muscle cells and adipocytes. *Nutr Metab (Lond)*. 2009;6:26.
 34. Hatazawa Y, Tadaishi M, Nagaike Y, Morita A, Ogawa Y, Ezaki O, et al. PGC-1alpha-mediated branched-chain amino acid metabolism in the skeletal muscle. *PLoS One*. 2014;9(3):e91006.
 35. Liang C, Curry BJ, Brown PL, Zemel MB. Leucine Modulates Mitochondrial Biogenesis and SIRT1-AMPK Signaling in C2C12 Myotubes. *J Nutr Metab*. 2014;2014:239750.
 36. Kamei Y, Hatazawa Y, Uchitomi R, Yoshimura R, Miura S. Regulation of Skeletal Muscle Function by Amino Acids. *Nutrients*. 2020;12(1).
 37. Vaughan RA, Garcia-Smith R, Gannon NP, Bisoffi M, Trujillo KA, Conn CA. Leucine treatment enhances oxidative capacity through complete carbohydrate oxidation and increased mitochondrial density in skeletal muscle cells. *Amino Acids*. 2013;45(4):901–11.

Figures

Experimental design

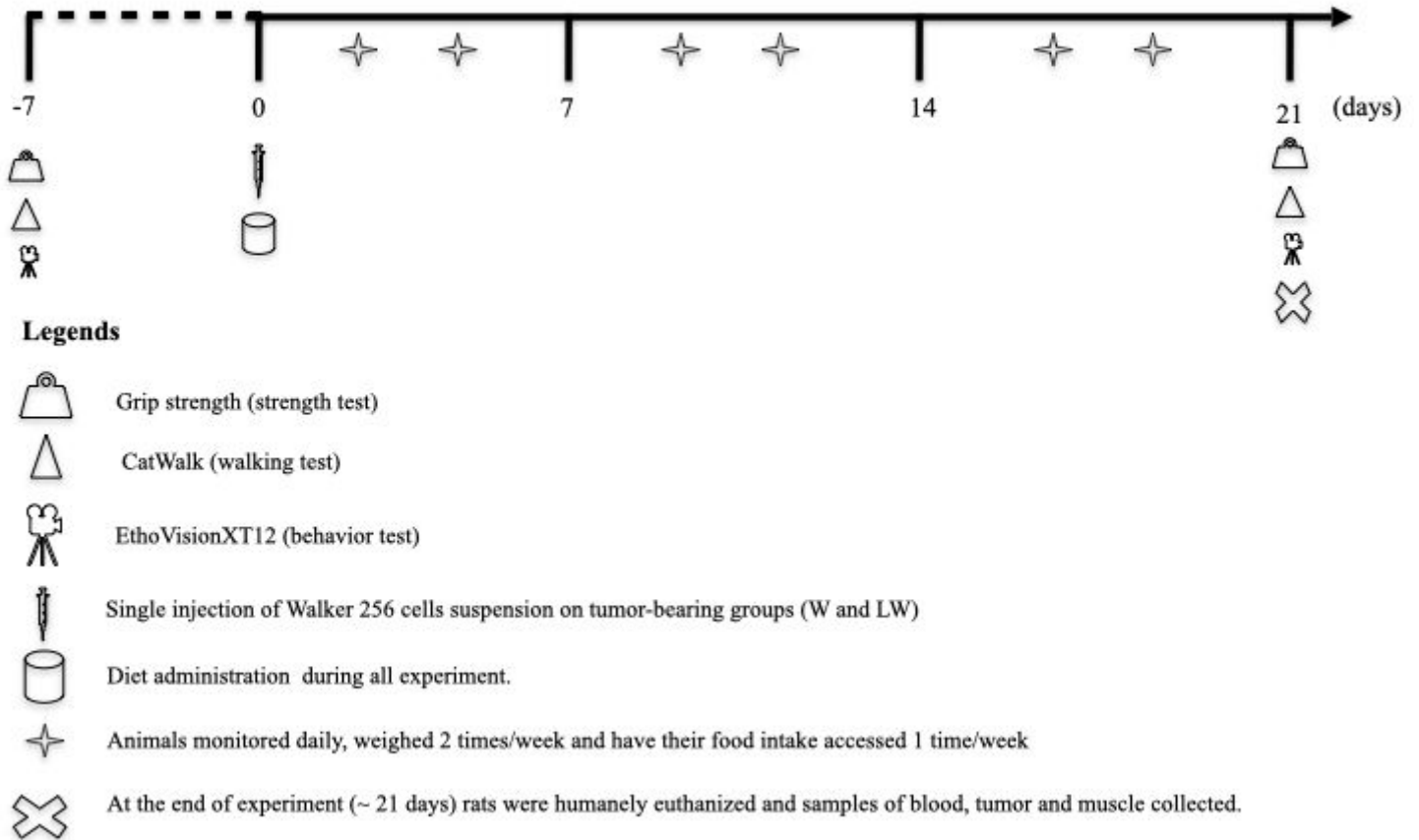


Figure 1

Experimental design. Male adult Wistar rats were monitored daily, weighed 3 times/week, and given food and water ad libitum. Food intake was measured once per week and the functional activities were accessed one week before (to access the health condition) and after approximately 18 days after tumor and diet administration (pre-agonic moment).

Walking test

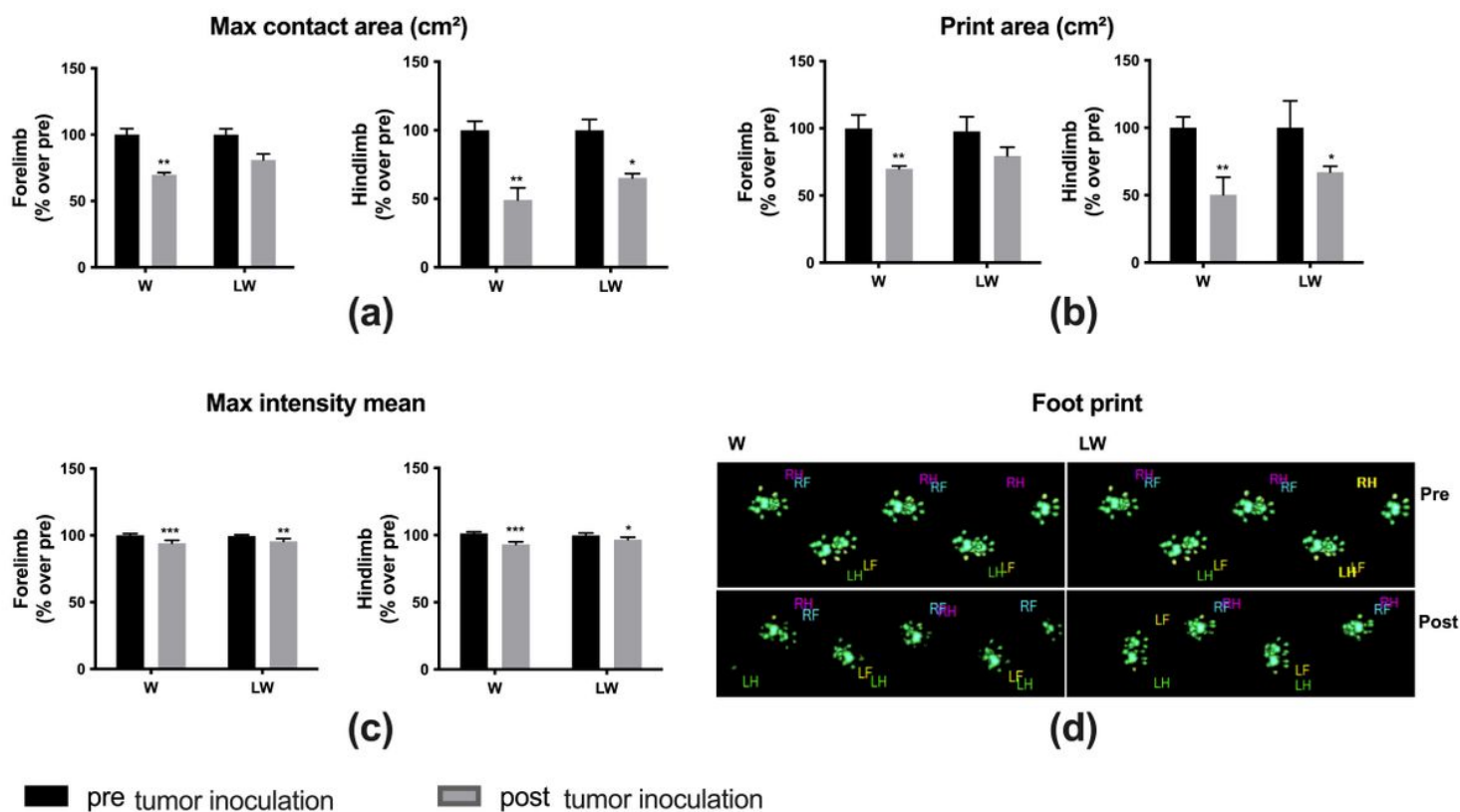


Figure 2

Catwalk functional (Walking test) parameters analyzed in tumor-bearing groups, fed or not the leu-cine-rich diet. (a): Maximum contact area (cm²) in forelimb and hindlimb paws; (b): Maximum intensity mean in forelimb and hindlimb paws; (c): Print area (cm²) in forelimb and hindlimb paws and (d): A representative image of 2D walking pattern of both W and LW groups before and after (end-point) tumor inoculation. Black bars represent the pre-tumor inoculation (health), and the grey bars represent the post-tumor inoculation (endpoint). The analysis was made using the same rats pre and post tumor evolution (n=6). *P<0.05, **P<0.01 and ***P<0.001 compared to the respectively pre-tumor moment by ANOVA followed by Tukey's test. RF – right front; LF – left front; RH – right hind; LH – left hind. The average of forepaws (RF and LF) was considered as forelimb, and the average of hind paws (RH and LH) were considered hindlimb. Graphics represent mean ± SEM. For details, see the Methods section.

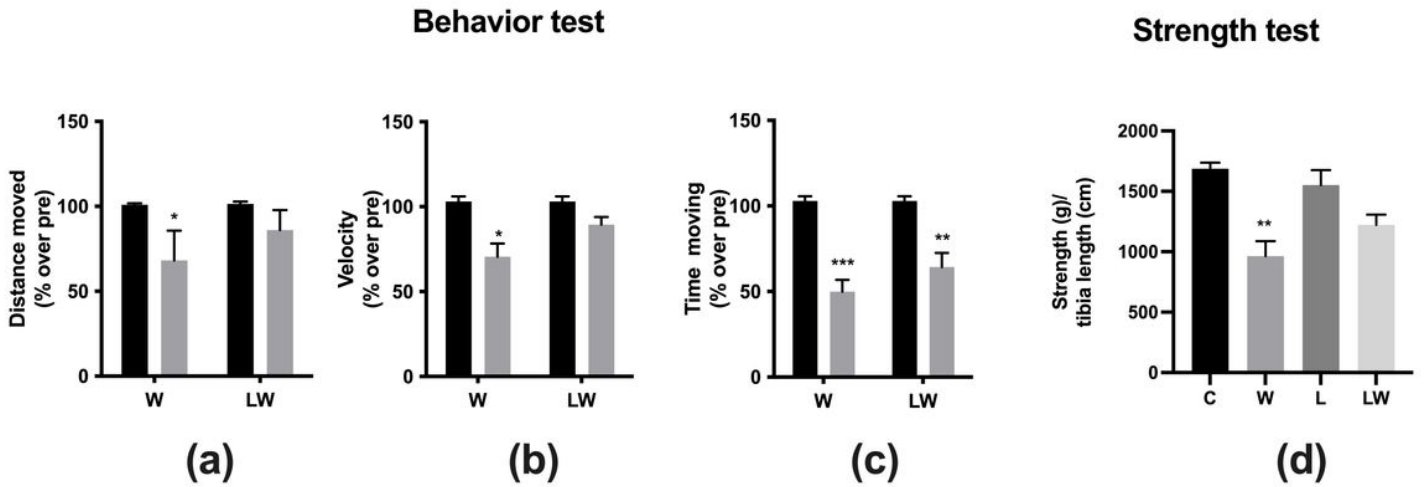


Figure 3

Evolution of behavior and muscle force in tumor-bearing groups, fed or not the leucine-rich diet. Echovision behavior parameters measured at nighttime. (a): Daily distance moved (cm), (b) Daily time moving (s) and (c) Velocity (cm/s). Black bars represent the pre-tumor inoculation, and the grey bars represent the post-tumor inoculation (endpoint). * $P < 0.05$, ** $P < 0.01$ and *** $P < 0.001$ over pre-tumor moment by ANOVA followed by Tukey's test. Strength test measurement. (d): Strength (g) normalized by tibia length (cm) measured at endpoint moment. ** $P < 0.01$ over the control (C) group by ANOVA followed by Tukey's test. Graphics represent mean \pm SEM. For details, see the Methods section.

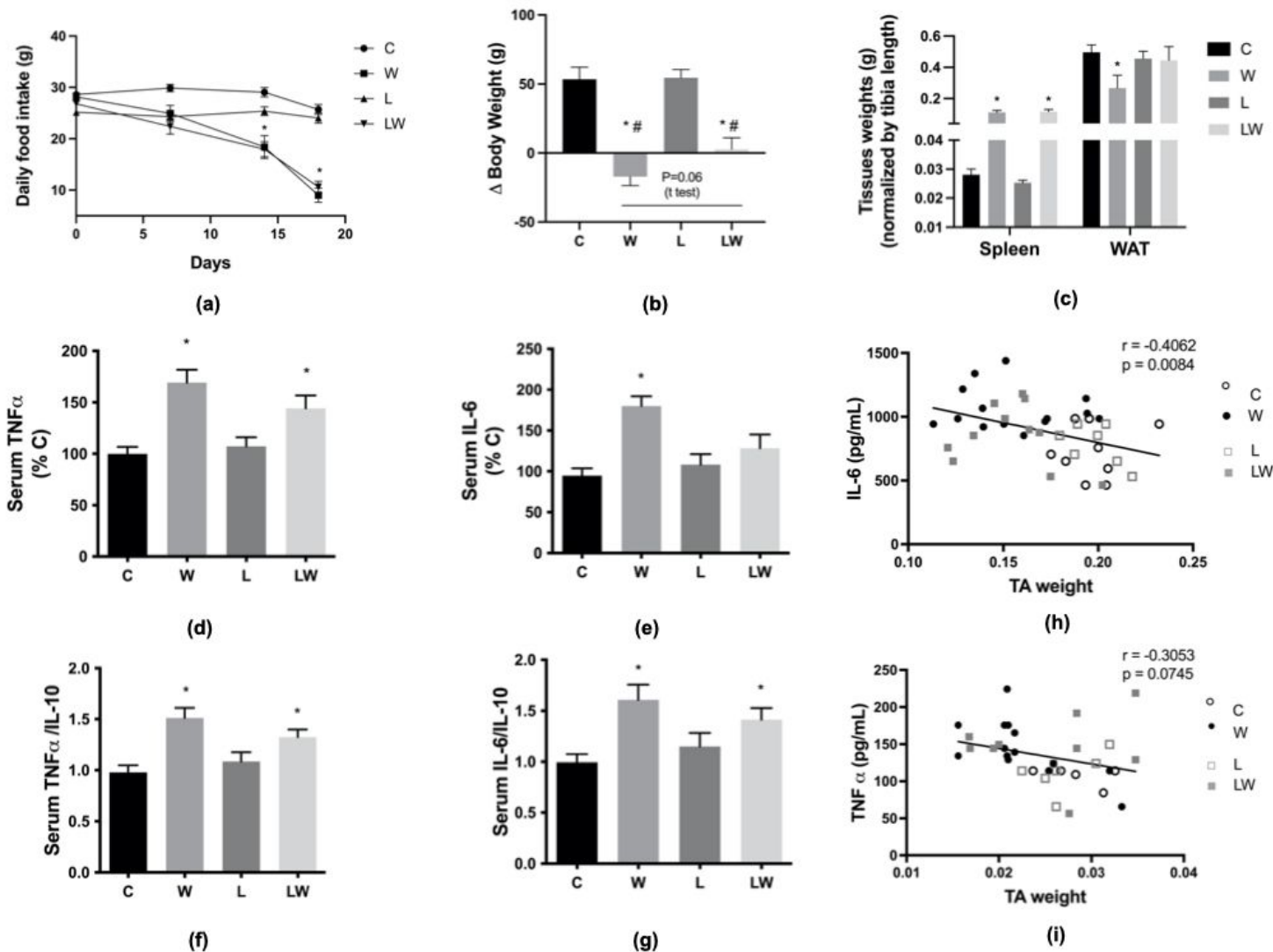


Figure 4

Morphological parameters (a). Daily food intake (g) during the experimentation protocol; (b). Delta body weight (g) for non-tumor bearing groups (C and L; calculated as final body weight-initial body weight) and tumor-bearing groups (W and LW; calculated as (final body weight-tumor weight)-initial body weight); (c) Relative tissue weights – spleen and WAT – white adipose tissue (perirenal) were calculated dividing the tissue weights by the respective tibia length and (d). Serum TNF- α level as a percentage of the C group; (e) Serum IL-6 concentration as a percentage of the C group; (f) Ratio of TNF- α /IL-10 and (g) Ratio of IL-6/IL-10; (h) correlation between IL-6 and tibialis anterior muscle and (i) correlation between TNF and tibialis anterior muscle. All serum cytokines were calculated as % over C group. $aP < 0.05$ vs C group by ANOVA followed by Tukey's test. Graphics represent mean \pm SEM. For details, see the Methods section.

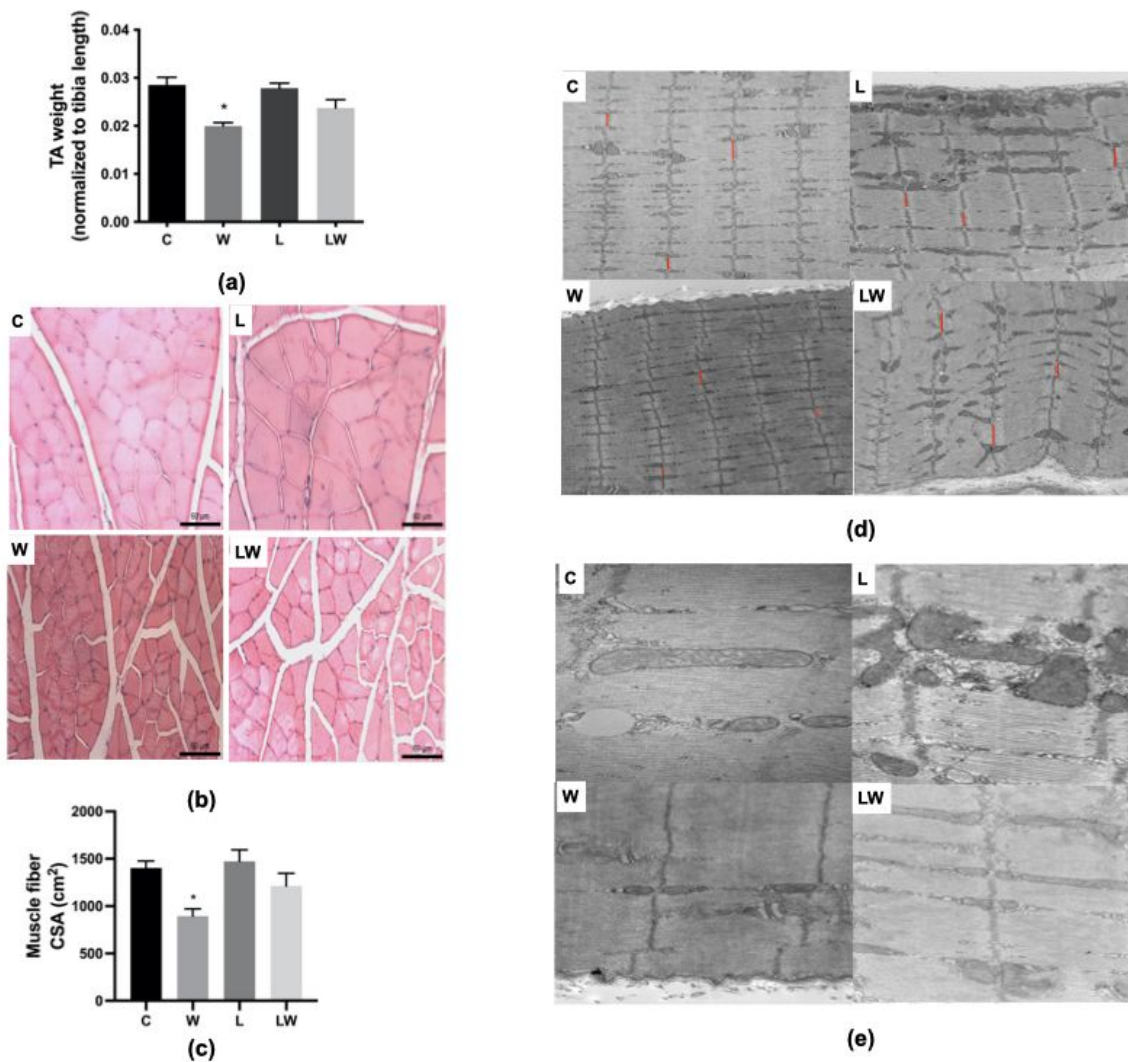


Figure 5

Morphometric and histological analyses of tibialis anterior muscle among the different experimental groups. (a) Tibialis anterior muscle (TA) corrected by tibia bone length. (b) Histological parameters, muscle tissue was included and stained by Hematoxylin Floxin staining muscle sections from C, L, W and LW groups (Scale bar: 60µm. Magnification 40x). (c) Measurements of myofiber cross-sectional area (µm²). (d) and (e) Transmission electron microscopy images. Magnification 10000x and 27800x, respectively. Red lines indicates sarcomere diameter. aP<0.05 vs C group by ANOVA followed by Tukey's test. Graphics represent mean ± SEM. For details, see the Methods section.

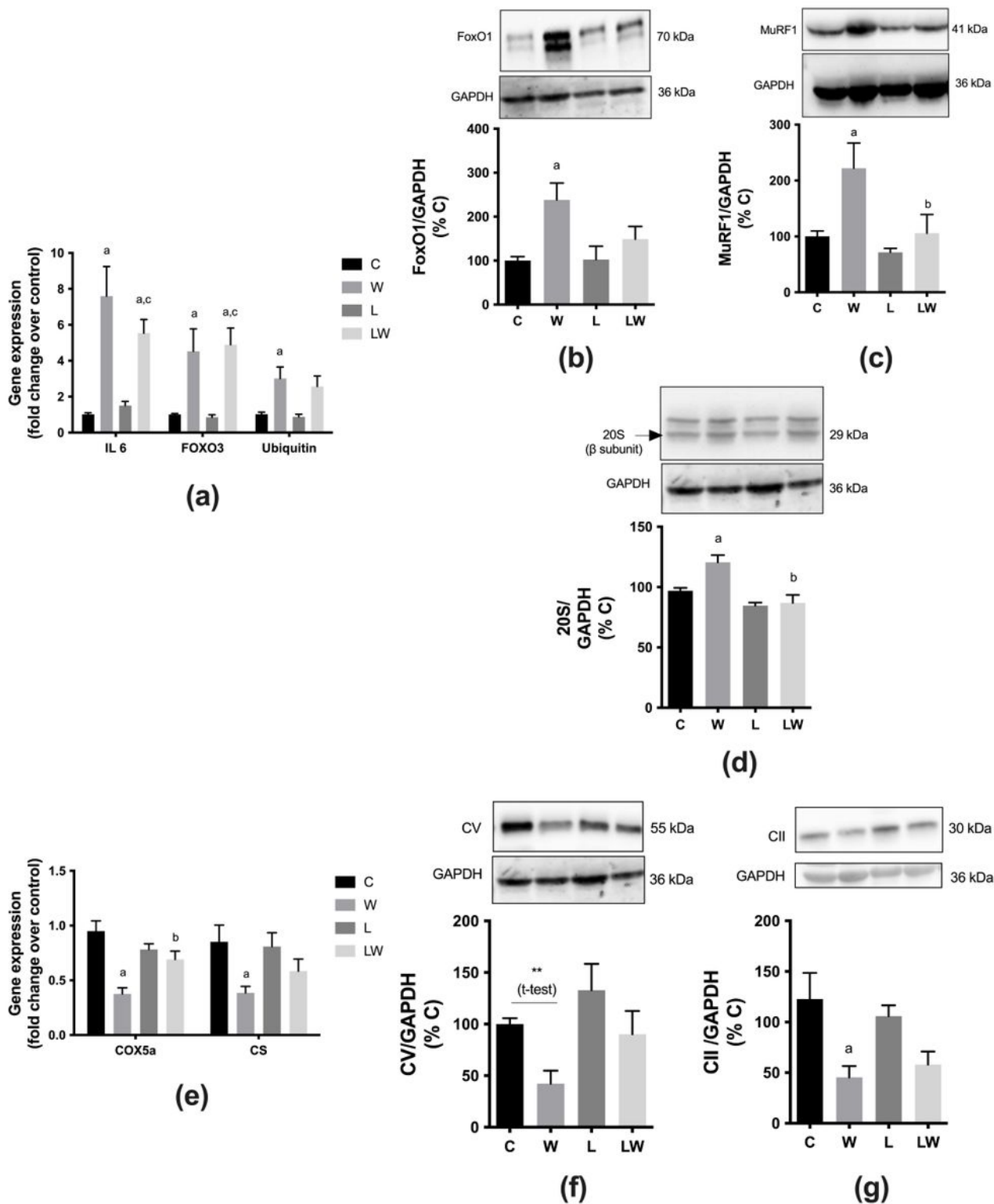


Figure 6

Muscular gene and protein expression among the different experimental groups. (a) Gene expression of IL6, FoxO3, and ubiquitin; (e) Gene expression of cyclooxygenase (COX)5a and citrate synthetase (CS). Protein expression. Western blot analysis images from (b) FoxO1, (c) MuRF1, and (d) 20S; (f) and (g) mitochondrial respiratory complexes: V (ATP5A [adenosine triphosphatase synthase 5A]) and II (SDHB [succinate dehydrogenase complex subunit B]) expressions in tibialis anterior muscle biopsies. Bar

graphs indicating western blot analysis representing values of band volume. GAPDH was used as a housekeeping protein. a $P < 0.05$ in comparison to C group; b $P < 0.05$ in comparison to W group and c $P < 0.05$ in comparison to L group by ANOVA followed by Tukey's test. Graphics represent mean \pm SEM. For details, see the Methods section.